

PHASE-SPACE CORRELATION IN STELLAR STREAMS OF THE MILKY WAY HALO: THE CLASH OF KSHIR AND GD-1¹

KHYATI MALHAN², RODRIGO A. IBATA³, RAYMOND G. CARLBERG⁴, MICHELE BELLAZZINI⁵, BENOIT FAMAËY³ AND NICOLAS F. MARTIN³

Accepted by The Astrophysical Journal Letters

ABSTRACT

We report the discovery of a 70° long stellar stream in the Milky Way halo, which criss-crosses the well known “GD-1” stream. We show that this new stellar structure (“Kshir”) and GD-1 lie at similar distance, and are remarkably correlated in kinematics. We propose several explanations for the nature of this new structure and its possible association with GD-1. However, a scenario in which these two streams were accreted onto the Milky Way within the same dark matter sub-halo seems to provide a natural explanation for their phase-space entanglement, and other complexities of this coupled-system.

Subject headings: dark matter - Galaxy: halo - globular clusters: general - stars: kinematics and dynamics

1. INTRODUCTION

Stellar streams are “fossil” remnants of accretion events that are formed by the tidal disruption of satellite systems as they accrete and begin to orbit in the gravitational potential of the host galaxy. More than 50 streams have been detected so far in the Milky Way halo (for e.g., Ibata et al. 2001; Belokurov et al. 2006; Grillmair 2009; Bernard et al. 2016; Balbinot et al. 2016; Myeong et al. 2017; Shipp et al. 2018; Malhan et al. 2018; Ibata et al. 2019). A large fraction of these old and metal poor structures are observed as narrow and one-dimensional structures (Grillmair & Carlin 2016), and are explained as stellar debris produced from globular clusters (GCs), that were perhaps brought in by their parent dark satellite galaxies during accretion (Renaud et al. 2017). Due mainly to their simple morphology and lack of associations with any other observed components of the stellar halo, the GC streams are generally modeled independently as simple GCs disrupting under the tidal force field of the host galaxy (e.g., Dehnen et al. 2004). The good match between observations and such simple models, in effect, also favours primeval models of GC formation - a scenario in which GCs originate from dark matter free gravitationally-bound gas clouds in the early Universe (Kravtsov & Gnedin 2005; Kruijssen 2014), and then later migrate into the host galaxy.

In this work, we report the discovery of a new Milky

Way stream, and find that it criss-crosses through the previously well known “GD-1” stream. We demonstrate that GD-1 and this new structure are highly correlated in distance and kinematics, and have similar stellar populations. We discuss the possible interpretations of the origin of this remarkable entangled system, and the potential implications of our results in dark matter and GC formation studies.

2. GD-1 AND ITS NEIGHBOUR

Ranging in heliocentric distance between $d_{\odot} \sim 8 - 12$ kpc, the GD-1 stream (Grillmair & Dionatos 2006) has been observed as an $\sim 80^{\circ}$ long (~ 12 kpc, Price-Whelan & Bonaca 2018), narrow (≈ 20 pc in physical width, Koposov et al. 2010), linear stellar structure. This GC stream is dynamically very cold (with a velocity dispersion of ≈ 1 km s⁻¹, Malhan & Ibata 2019, MI19 hereafter) and is remarkably metal deficient ([Fe/H] = -2.24 ± 0.21 dex).

Fig 1a shows the density map in the region around GD-1 that we obtained by processing the entire ESA/Gaia DR2 dataset (Gaia Collaboration et al. 2018; Lindegren, L. et al. 2018) with the STREAMFINDER software (Malhan & Ibata 2018; Malhan et al. 2018; Ibata et al. 2019). Briefly, STREAMFINDER works by examining every star in the Gaia survey in turn, sampling the possible orbits consistent with the observed photometry and kinematics, and finding the maximum-likelihood stream solution given a contamination model and a stream model. As in Malhan et al. (2018), we de-reddened the survey using the Schlegel et al. (1998) dust maps, and kept only those stars with (de-reddened) $G_0 < 19.5$ to ensure homogeneous depth over the sky. The stream width parameter in the search algorithm was set to 50 pc, and we used single stellar population (SSP) template models from the PARSEC stellar tracks library (Bressan et al. 2012) of age 12.5 Gyr, and scanned a range of metallicities of [Fe/H] = $-2.2, -2.0, -1.6, -1.2, -0.8, -0.4$. For each processed star, we thus obtained 6 stream solutions, corresponding to the 6 trial SSP metallicity values, and we accepted the solution that yielded the highest likeli-

khyati.malhan@fysik.su.se

¹Based on observations obtained at the Canada-France-Hawaii Telescope (CFHT) which is operated by the National Research Council of Canada, the Institut National des Sciences de l’Univers of the Centre National de la Recherche Scientifique of France, and the University of Hawaii.

²The Oskar Klein Centre for Cosmoparticle Physics, Department of Physics, Stockholm University, AlbaNova, 10691 Stockholm, Sweden

³Université de Strasbourg, CNRS, Observatoire Astronomique de Strasbourg, UMR 7550, F-67000 Strasbourg, France

⁴Department of Astronomy & Astrophysics, University of Toronto, Toronto, ON M5S 3H4, Canada

⁵INAF - Osservatorio di Astrofisica e Scienza dello Spazio, via Gobetti 93/3, 40129 Bologna, Italy

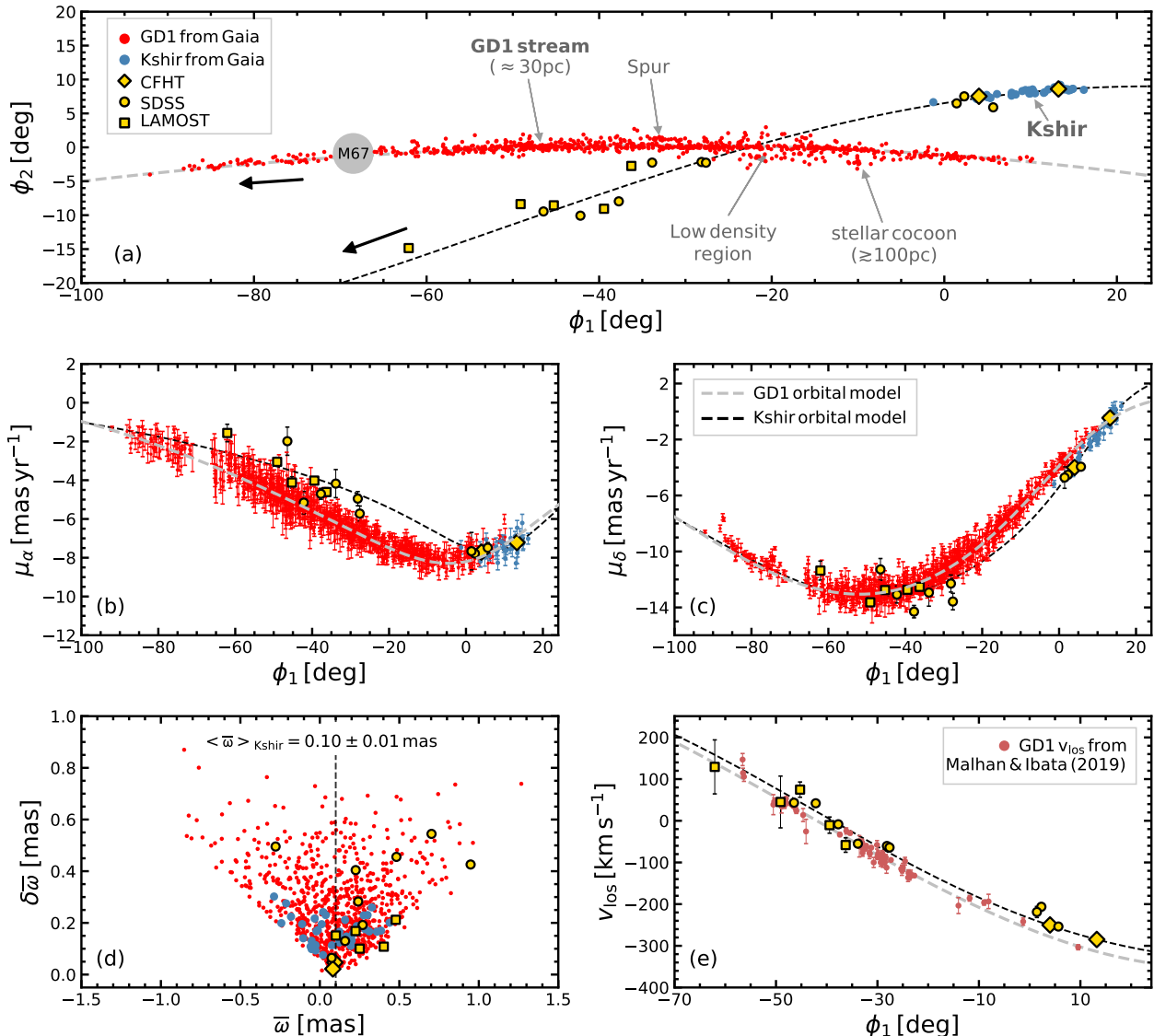


FIG. 1.— Spatial and kinematic distribution of GD-1 and Kshir. a: Sky position in $\phi_1 - \phi_2$ coordinates, which are a rotated celestial system aligned along GD-1. The narrow GD-1 (≈ 30 pc wide) can be immediately spotted along $\phi_2 \sim 0^\circ$. Some additional features can also be observed, such as the low density regions along the stream, the “spur” component and the “cocoon” component ($\gtrsim 100$ pc wide). An arc-like structure can be seen at $(\phi_1, \phi_2) \sim (10^\circ, 8^\circ)$, which we refer to as “Kshir”. Spectroscopically confirmed members for Kshir are shown in yellow. The region of sky containing the foreground open cluster M67 ($d_\odot \sim 0.9$ kpc) was masked out prior to the running of the STREAMFINDER. The bold arrows indicate the direction of motion of the two streams. Panels b, c and d show, respectively, proper motion in μ_α , μ_δ , and parallax \bar{w} , as a function of ϕ_1 . Panel e shows the heliocentric line-of-sight velocities v_{los} of the members of GD-1 (pink) and Kshir (yellow). The derived orbits of the two structures are shown in each panel, and can be seen to be very similar.

hood. GD-1 appears as a completely distinguished structure in our STREAMFINDER maps, as shown in Fig 1a. It transpires that the best orbital solution for 88% of the GD-1 stars is obtained with an SSP template with metallicity $[\text{Fe}/\text{H}] = -2.2$, similar to the measured $[\text{Fe}/\text{H}]$ value (MI19)⁶. We also set the stream-detection significance to $> 8\sigma$, which means that at the position of every star, the algorithm finds that there is a $> 8\sigma$ significance for there to be a stream-like structure. This results in a sample of 811 stars in the region around GD-1 that are shown in Fig 1a (red and blue points). The region of the sky containing the foreground open cluster M67 was

⁶ The value 88% corresponds to the fraction of stars (identified as GD-1) obtained as stream solution using that particular $[\text{Fe}/\text{H}]$ model.

masked out prior to running the STREAMFINDER.

Fig 1a reveals the complex structure that surrounds the thin GD-1 stream (shown with red points). The plot is presented in $\phi_1 - \phi_2$ coordinates (Koposov et al. 2010), which align along GD-1. A narrow component of GD-1 (≈ 30 pc wide) can be readily seen along $\phi_2 \approx 0^\circ$, enveloped by a broad and diffuse structure ($\gtrsim 100$ pc wide). This extended component was previously reported in Malhan et al. (2019), and was referred to as the *cocoon* component. The code also tentatively detected the previously-known low density regions and the “spur” component (Price-Whelan & Bonaca 2018).

The present study focuses on the detection of the arc-like feature that is conspicuously visible in Fig 1a at $(\phi_1, \phi_2) \approx (10^\circ, 8^\circ)$, skirting almost parallel to GD-

1 (shown with blue points). We refer to this structure as “Kshir”⁷. Based on the orbital analysis of the *STREAMFINDER* code, we note that both Kshir and GD-1 are found by the algorithm with similar values of the z -component of angular momentum (L_z) and energy (E). In particular, the algorithm (in the adopted potential model) estimates $(L_z, E)_{\text{GD1}} = (2900 \pm 800 \text{ kpc km s}^{-1}, -88000 \pm 19000 \text{ km}^2 \text{ s}^{-2})$ and $(L_z, E)_{\text{Kshir}} = (3200 \pm 600 \text{ kpc km s}^{-1}, -89000 \pm 13000 \text{ km}^2 \text{ s}^{-2})$. This indicates that they are, perhaps, part of the same coherent group and share a common origin. The *STREAMFINDER* detects a total of 42 stars for the Kshir stream from Gaia DR2. We realized that one of these stars fortuitously had a spectroscopic observation in the SDSS/Segue (DR10, Yanny et al. 2009), from which we obtained the metallicity ($[\text{Fe}/\text{H}]$) and line-of-sight velocity (v_{los}) values. A further 2 stars were observed with the ESPaDOnS high-resolution spectrograph on the Canada-France-Hawaii Telescope (CFHT) in service mode, as a part of our own follow up program. The data were reduced with the Libre-ESPRIT pipeline (Donati et al. 1997), and we measured the stars’ velocities using the *fxcor* command in IRAF. The chemical abundances of the stars (which are part of a much larger sample of streams) are currently being analysed, and will be presented in a later contribution. These 3 stars are mentioned in the top rows of Table 1 and are also shown in Fig 1. Kshir is already visible in Fig 1 of Malhan et al. (2019), however was not focussed upon, as we previously lacked spectroscopic measurements for this structure.

We used the Kshir orbit model, derived in Section 3, to find additional member stars that lie along its trajectory. To this end, we used the 5D astrometric measurements (that came from Gaia DR2 for blue stars shown in Fig 1a), in combination with the aforementioned 3 velocity measurements, for Kshir stars to obtain a solution for its orbit. This orbit-fitting procedure is detailed in Section 3. We now assume that we possess a reasonable orbital representation of the Kshir structure.

To identify additional spectroscopic members of Kshir, we first created a special dataset by cross-matching the Gaia DR2 catalogue with the SDSS (Yanny et al. 2009) and LAMOST DR4 (Zhao et al. 2012) spectroscopic datasets, and selected those stars with Gaia colors in the range $(0.40 < [G_{\text{BP}} - G_{\text{RP}}]_0 < 1.60)$, with magnitude ($G_0 < 20$), and with spectroscopic metallicity $[\text{Fe}/\text{H}] < -0.5$ dex. We further selected those stars that lie within 3σ of Kshir’s orbit model in the observed parallax ($\bar{\omega}$), proper motion (μ_α, μ_δ), and line of sight velocity v_{los} space, and within ~ 300 pc perpendicular to the orbit (which defines the maximum possible stream width). We do not make any additional selections in photometry and $[\text{Fe}/\text{H}]$ at this stage, since we do not a priori know the properties of Kshir’s stellar population. This 6-dimensional selection yields a total of 13 stars (8 from SEGUE and 5 from LAMOST), that represent additional Kshir’s candidate members. These stars were not previously identified by the *STREAMFINDER* due to their lower contrast. We verified that the expected contamination from a smooth halo model (as predicted by the

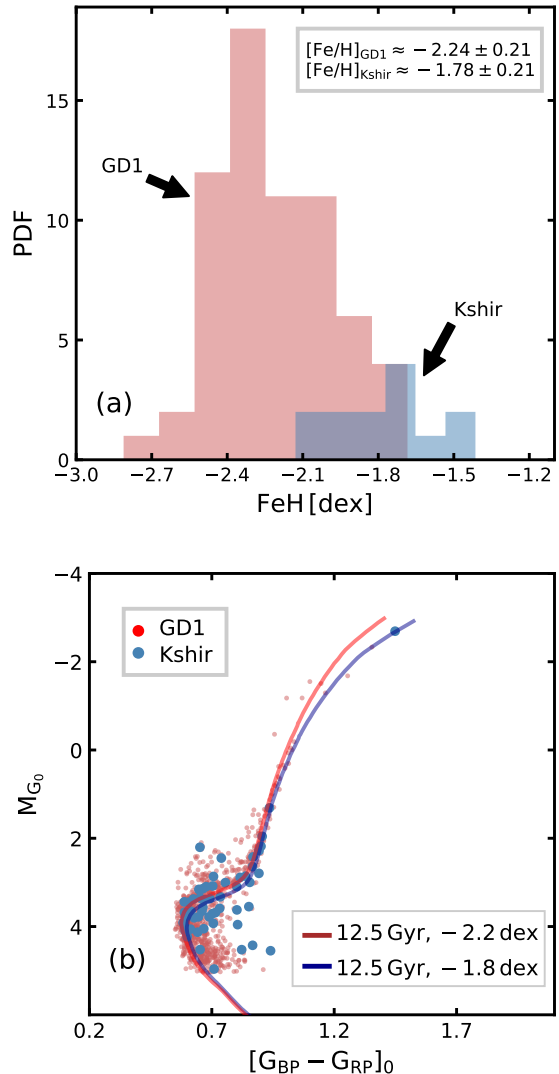


FIG. 2.— Metallicity and photometry of GD-1 and Kshir. *Top panel*: $[\text{Fe}/\text{H}]$ distribution of spectroscopically-confirmed members of GD-1 (red) and Kshir (blue) stars. *Bottom panel*: Gaia (de-reddened) color-magnitude diagram of all member stars of Kshir and GD-1, previously shown in Fig 1. The absolute magnitude were then obtained by correcting the observed magnitude value for the orbital distance of each star. Two SSP template models, corresponding to the mean metallicity values of the streams, are also shown.

GUMS simulation, Robin et al. 2012) along Kshir’s orbit is nearly zero.

The combined phase-space properties of the stellar members of Kshir and GD-1 are plotted in Fig 1a-e (along with the spectroscopically confirmed members for Kshir that are shown in yellow). One readily observes that GD-1 and Kshir intersect spatially, at $\phi_1 \approx -20^\circ$, and are also strongly entangled in proper motion space. In the v_{los} panel, the stars corresponding to GD-1 refer to the spectroscopically-confirmed members inventoried in MI19. It can be easily discerned that Kshir stars lie quite close to the GD-1 stars even in v_{los} space. The orbit of GD-1 (obtained from MI19) and Kshir look very similar in every phase-space dimension, and Kshir’s orbit predicts similar v_{los} gradient along the length of the stream as observed for GD-1, with an almost constant offset of

⁷ In Hindu mythology, *Kshir* refers to a water body made of milk.

$\approx 20 \text{ km s}^{-1}$. We caution that the lack of stars between $\phi_1 \sim -25^\circ$ to 0° in Kshir may either be physical in origin, or could be due to the selection effect of the SEGUE and LAMOST surveys; however is hard to quantify at this stage. Also note that the leading part of Kshir (dominated by 6D members) appears much wider than the trailing part. This result could be specific to the criteria adopted here to select Kshir stars, and future analysis (with a larger sample size) should better characterise the structural morphology of this stream.

The uncertainty-weighted average mean parallax for Kshir (for blue points in Fig 1) is $\langle \bar{\omega} \rangle = 0.10 \pm 0.01 \text{ mas}$, i.e. $\sim 10 \text{ kpc}$ in distance, which is similar to the distance of the GD-1 orbit in the same range of ϕ_1 ($\sim 8.5 \text{ kpc}$). The metallicities of Kshir and GD-1 are compared in Figure 2a. We find $[\text{Fe}/\text{H}] = -1.78 \pm 0.21 \text{ dex}$ for Kshir, implying that it is systematically more metal-rich than GD-1 by $\sim 0.4 \text{ dex}$. On performing a two-sample Kolmogorov-Smirnov (KS) test for the null hypothesis that the two $[\text{Fe}/\text{H}]$ samples are drawn from the same distribution, the resulting probability was found to be $p_{\text{KS}} = 3.78 \times 10^{-5}$: indicating that the hypothesis can be rejected at the 4σ level. Their stellar populations are compared in Figure 2b, where we display the magnitudes corrected for the distance of the stars, as estimated from the orbit models at the corresponding value of ϕ_1 . While the CMDs appear similar, the metallicity distributions suggest that the stellar populations are not identical.

3. ORBIT

In MI19 we implemented an orbit-fitting procedure to a sample of GD-1 stars in order to constrain the gravitational potential of the Milky Way. This orbit is shown in Fig 1. Here we fix the Galactic potential model derived in that study (which has a circular velocity at the Solar radius of $V_{\text{circ}}(R_\odot) = 244 \text{ km s}^{-1}$, and a density flattening of the dark halo as $q_p = 0.82$), and follow a similar procedure (with identical likelihood function) as that presented in MI19 to fit the orbit of Kshir.

We used the 42 Kshir stars identified by the STREAMFINDER (shown as blue points in Fig 1), in combination with the 3 velocity measurements from CFHT and SEGUE that are available for those targets⁸. The best-fit orbit for Kshir is shown in Fig 1. We find its orbit to be more circular than that of GD-1 (see Fig 3), but with $L_z (\sim 2700 \pm 200 \text{ kpc km s}^{-1})$ comparable to that of GD-1 ($L_z \sim 2950 \text{ kpc km s}^{-1}$, MI19). The difference in the L_z values stems from the aforementioned offset in the kinematic measurements between the two structures.

These orbits suggest that the last closest approach between Kshir and GD-1 occurred $\sim 1.7 \text{ Gyr}$ ago with an impact parameter of $\sim 1 - 2 \text{ kpc}$, although we caution that these values depend on the assumed Galactic potential model.

4. DISCUSSION AND CONCLUSIONS

We have presented the discovery of a new stream structure, referred to as ‘‘Kshir’’, which criss-crosses the well

⁸ We dealt with the missing v_{los} information for the remaining 39 stars by setting them all to $v_{\text{los}} = 0 \text{ km s}^{-1}$, but with a Gaussian uncertainty of 10^4 km s^{-1} . The results are almost identical if instead an uncertainty of 10^3 km s^{-1} is assumed. The choice of adopting a 10^4 km s^{-1} uncertainty is effectively imposing a prior that the stars must be located in the local universe.

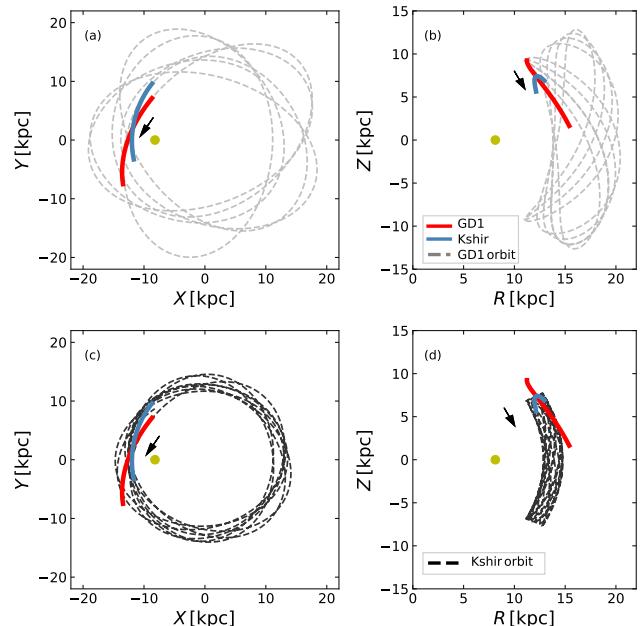


FIG. 3.— The orbital trajectories of GD-1 and Kshir in the Galactocentric Cartesian system. *Top panels:* GD-1’s orbit (silver). For perspective, the current locations of GD-1 (red) and Kshir (blue) are also shown. The Galactic centre lies at the origin and the Sun (yellow dot) is at $(X, Y, Z) = (-8.122, 0, 0) \text{ kpc}$. The orbit was integrated backwards in time for 3 Gyr. The arrows represent the direction of motion of the structures. *Bottom panels:* As above, but showing Kshir’s orbit (black).

TABLE 1
SPECTROSCOPICALLY CONFIRMED MEMBERS OF KSHIR. THE SKY COORDINATES ARE FROM GAIA DR2, WHILE THE v_{los} AND $[\text{Fe}/\text{H}]$ ARE MEASUREMENTS FROM CFHT (C), SEGUE (S) AND LAMOST (L).

RA J2000 [deg]	Dec J2000 [deg]	v_{los} [km s^{-1}]	$[\text{Fe}/\text{H}]$ [dex]	Source
201.53579	67.28841	-206.32	-1.78	S
205.87918	67.57526	-249.95	—	C
230.38107	68.16672	-284.78	—	C
147.96434	9.65499	129.28	-1.56	L
150.32399	23.73448	45.09	-1.76	L
153.05409	25.1087	43.33	-1.74	S
153.10830	26.59341	74.75	-1.41	L
154.73641	37.16519	-58.23	-1.47	L
156.31086	39.28787	-54.95	-1.94	S
156.64035	27.9157	41.96	-1.71	S
157.84587	30.59822	-10.42	-2.1	L
158.26272	32.5852	-8.47	-1.67	S
161.53675	43.45613	-60.52	-2.13	S
162.14438	43.73839	-64.03	-1.99	S
199.92916	66.09159	-218.86	—	S
210.43905	66.11245	-253.76	-1.83	S

studied GD-1 stream on the sky, lies at similar distance, and possesses very similar kinematics (Fig 1). Moreover, we find Kshir to be also an old and metal poor structure ($[\text{Fe}/\text{H}] \approx -1.78 \pm 0.21 \text{ dex}$), though slightly more metal rich than GD-1 (Fig 2). Fig 1a shows that Kshir’s orbit intersects GD-1 at $\phi_1 \sim -20^\circ$, which is also the location of the tentative ‘‘gap’’ present along GD-1 (Price-Whelan & Bonaca 2018).

Such a phase-space entanglement in GC streams has

not previously been reported. This makes the nature and origin of Kshir, and its possible association with GD-1, very intriguing. We consider below three explanations for the observed correlation.

A) Orbital wraps of same structure. If Kshir and GD-1 stemmed from the same GC progenitor, then the observed configuration could be due to the presence of different orbital wraps. In this case, Kshir might possibly be a portion of the GD-1 stream that is wrapped by $\sim 360^\circ$ (or multiples thereof). The fact that Kshir does not simply line up along the orbit of GD-1 (Fig 3) argues against this possibility, although we stress that this result is valid only for the adopted potential derived in MI19. It is possible that other, more complex, Galactic potentials could simultaneously fit extant data and allow Kshir to be a simple wrap of GD-1. Nevertheless, this scenario seems unlikely, due to the difference in the chemical composition of the two structures. This consideration does not completely rule out the scenario, however, since it is possible that the progenitor satellite may have possessed a radial metallicity gradient (like, e.g., ω Cen, Johnson & Pilachowski 2010). If tides act slowly, they disrupt the progenitor by progressively removing its outskirts, which can then result in the tidal stream possessing metallicity variations along its length.

B) A chance alignment of two independent GCs. It is possible that Kshir and GD-1 are tidal debris of two unassociated GCs. However, given the vast phase-space volume of the Milky Way, such a degree of phase-space overlapping of two unrelated stellar substructures is a low likelihood event. To obtain an estimate of the corresponding probability, we implemented the following test. Employing the `Halotools` package (Hearin et al. 2017), we randomly generated a phase-space distribution in an isotropic NFW halo profile (Navarro et al. 1996), with a virial mass of $1.28 \times 10^{12} M_\odot$ (Watkins et al. 2019). From this distribution we calculated the probability that two randomly-drawn tracer particles at the distance of the objects of interest have similar orbits. Concretely, we drew 10^4 random pairs of particles in the Galactocentric distance range between 13–15 kpc and counted the number of times these pairs possessed a relative difference in the z -component of angular momentum of $\Delta L_z < 300 \text{ kpc km s}^{-1}$, and with relative difference in the energy per unit mass of $\Delta E < 10000 \text{ km}^2 \text{ s}^{-2}$ (as is the case of Kshir and GD-1). We found this probability to be ~ 0.007 . This implies that if Kshir and GD-1 are unrelated, then the probability of their chance phase-space alignment is $< 1\%$.

C) Common origin. The degree of phase-space correlation as we observe for Kshir and GD-1 is possible if the two structures originated from a common parent sub-halo that was accreted onto the Milky Way. Under this scenario, the stellar contents of the sub-halo system would be deposited on very similar orbits. Cosmological simulations show that GCs that evolve within their dark sub-halos, and later accrete into the host halo, give rise to stellar streams that possess substantial morphological complexity (Carlberg 2018a). This often results in secondary stellar components that accompany the primary GC stream track (see figures in Carlberg 2018b), with the overall structure remaining kinematically coherent (much like we see here for Kshir and GD-1). In addi-

tion to this, the cosmological simulations further show that the accreted GC streams should lie embedded in broader and dispersed star streams. The reason for this is that the primary stream (which is thin and dense) that survives to the present day is formed once the GC escapes the parent sub-halo and is deposited into the main halo; whereas the wider stellar component enveloping the thin stream is the relic of the stars that were continually removed from the GC while it remained in its parent dark sub-halo. Evidence for this broader stream in GD-1 (labelled “cocoon” in Fig 1a) was already reported in Malhan et al. (2019). Moreover, these simulations also show criss-crossing of streams from separate GCs that formed in a single sub-halo; although an implication is that the sub-halo must be sufficiently massive to host multiple GCs. Therefore, both the Kshir structure and the existence of “cocoon” in neighbourhood of GD-1 strengthen the case for this “accretion” scenario. Further, the measured difference in metallicity between the two structures argues against a single GC progenitor, although again the constraint is not entirely conclusive (partially because the progenitor could have possessed a radial metallicity gradient). Alternatively, GD-1 and Kshir may correspond to stellar debris produced from either different GC members of the same dark sub-halo, or Kshir may perhaps be debris of the stellar component of the dwarf galaxy that was stripped off during the accretion. A detailed chemical abundance analysis will help to distinguish between these possibilities. Assuming the hypothesized dwarf galaxy hosted a metal poor GC and a field population with $[\text{Fe}/\text{H}]_{\text{field}} \sim -1.78$ dex, we estimate its total stellar mass as $M_* \sim 10^5 M_\odot$ (using the Stellar Mass-Stellar Metallicity Relation from Kirby et al. 2013), implying $M_{\text{halo}} \sim 10^{8-9} M_\odot$ (from stellar-to-halo-mass relation from Read et al. 2017). This makes the progenitor very similar to Eridanus II dwarf (Bechtol et al. 2015) which is also known to host a single GC (Crnojević et al. 2016). However, if the dwarf hosted two GCs (and assuming the field stars to be at least as metal-rich as the GCs), then the above quoted mass values in this case would represent typical lower bounds. None of the luminous satellites have orbits close to GD-1’s trajectory (Bonaca et al. 2019b), however, a future detection of a faint disrupting galaxy along GD-1’s/ Kshir’s orbit would serve as “smoking gun” evidence for the proposed accretion scenario. On the other hand, its lack supports a scenario where Kshir and GD-1 were perhaps accreted as GC(s) within an empty dark sub-halo.

The stellar streams of the Milky Way have unexpectedly revealed their rather complex morphologies (Price-Whelan & Bonaca 2018; Malhan et al. 2019; Bonaca et al. 2019a), which presents evidence for a formation mechanism that appears incompatible with a simple tidal disruption model. Modeling GD-1, particularly in light of these new observational constraints, may allow us to develop an understanding of the origins of these recently-found complexities in this well-studied system. This may also allow us to examine whether some GCs can form in otherwise empty CDM sub-halos before, or shortly after re-ionization began (e.g., Peebles 1984; Mashchenko & Sills 2005; Ricotti et al. 2016), giving rise to stream structures that exhibit multiple structural components. A detailed dynamical and

chemical analysis of GD-1 and Kshir may potentially be useful in distinguishing in-situ and accreted GC stream, and in probing the initial conditions of the dark sub-halo within which they came.

We thank the staff of the CFHT for taking the ES-PaDONs data used here, and for their continued support throughout the project.

The authors would like to acknowledge the constructive set of comments from the anonymous reviewer. We further thank Monica Valluri and Justin I. Read for helpful conversations. K.M. acknowledges support by the Vetenskapsrådet (Swedish Research Council) through contract No. 638-2013-8993 and the Oskar Klein Centre for Cosmoparticle Physics, and is grateful for the hospitality received at Observatoire Astronomique de Strasbourg (UdS) where part of the work was performed.

This work has made use of data from the European Space Agency (ESA) mission *Gaia* (<https://www.cosmos.esa.int/gaia>), processed by the *Gaia* Data Processing and Analysis Consortium (DPAC, <https://www.cosmos.esa.int/web/gaia/dpac/consortium>). Funding for the DPAC has been provided by national institutions, in particular the institutions participating in the *Gaia* Multilateral Agreement.

Guoshoujing Telescope (the Large Sky Area Multi-Object Fiber Spectroscopic Telescope LAMOST) is a National Major Scientific Project built by the Chinese

Academy of Sciences. Funding for the project has been provided by the National Development and Reform Commission. LAMOST is operated and managed by the National Astronomical Observatories, Chinese Academy of Sciences.

Funding for SDSS-III has been provided by the Alfred P. Sloan Foundation, the Participating Institutions, the National Science Foundation, and the U.S. Department of Energy Office of Science. The SDSS-III web site is <http://www.sdss3.org/>.

SDSS-III is managed by the Astrophysical Research Consortium for the Participating Institutions of the SDSS-III Collaboration including the University of Arizona, the Brazilian Participation Group, Brookhaven National Laboratory, Carnegie Mellon University, University of Florida, the French Participation Group, the German Participation Group, Harvard University, the Instituto de Astrofísica de Canarias, the Michigan State/Notre Dame/JINA Participation Group, Johns Hopkins University, Lawrence Berkeley National Laboratory, Max Planck Institute for Astrophysics, Max Planck Institute for Extraterrestrial Physics, New Mexico State University, New York University, Ohio State University, Pennsylvania State University, University of Portsmouth, Princeton University, the Spanish Participation Group, University of Tokyo, University of Utah, Vanderbilt University, University of Virginia, University of Washington, and Yale University.

REFERENCES

- Balbinot, E., Yanny, B., Li, T. S., et al. 2016, *ApJ*, 820, 58
 Bechtol, K., Drlica-Wagner, A., Balbinot, E., et al. 2015, *ApJ*, 807, 50
 Belokurov, V., Zucker, D. B., Evans, N. W., et al. 2006, *ApJ*, 642, L137
 Bernard, E. J., Ferguson, A. M. N., Schlafly, E. F., et al. 2016, *MNRAS*, 463, 1759
 Bonaca, A., Conroy, C., Price-Whelan, A. M., & Hogg, D. W. 2019a, *ApJ*, 881, L37
 Bonaca, A., Hogg, D. W., Price-Whelan, A. M., & Conroy, C. 2019b, *ApJ*, 880, 38
 Bressan, A., Marigo, P., Girardi, L., et al. 2012, *MNRAS*, 427, 127
 Carlberg, R. G. 2018a, *ApJ*, 861, 69
 —. 2018b, arXiv e-prints, arXiv:1811.10084
 Crnojević, D., Sand, D. J., Zaritsky, D., et al. 2016, *The Astrophysical Journal*, 824, L14
 Dehnen, W., Odenkirchen, M., Grebel, E. K., & Rix, H.-W. 2004, *The Astronomical Journal*, 127, 2753
 Donati, J.-F., Semel, M., Carter, B. D., Rees, D. E., & Collier Cameron, A. 1997, *MNRAS*, 291, 658
 Gaia Collaboration, Brown, A. G. A., Vallenari, A., et al. 2018, *A&A*, doi:10.1051/0004-6361/201833051
 Grillmair, C. J. 2009, *ApJ*, 693, 1118
 Grillmair, C. J., & Carlin, J. L. 2016, in *Astrophysics and Space Science Library*, Vol. 420, Tidal Streams in the Local Group and Beyond, ed. H. J. Newberg & J. L. Carlin, 87
 Grillmair, C. J., & Dionatos, O. 2006, *ApJ*, 643, L17
 Hearin, A. P., Campbell, D., Tollerud, E., et al. 2017, *AJ*, 154, 190
 Ibata, R., Irwin, M., Lewis, G. F., & Stolte, A. 2001, *ApJ*, 547, L133
 Ibata, R. A., Malhan, K., & Martin, N. F. 2019, *ApJ*, 872, 152
 Johnson, C. I., & Pilachowski, C. A. 2010, *ApJ*, 722, 1373
 Kirby, E. N., Cohen, J. G., Guhathakurta, P., et al. 2013, *ApJ*, 779, 102
 Koposov, S. E., Rix, H.-W., & Hogg, D. W. 2010, *ApJ*, 712, 260
 Kravtsov, A. V., & Gnedin, O. Y. 2005, *ApJ*, 623, 650
 Kruijssen, J. M. D. 2014, *Classical and Quantum Gravity*, 31, 244006
 Lindgren, L., Hernandez, J., Bombrun, A., et al. 2018, *A&A*, doi:10.1051/0004-6361/201832727
 Malhan, K., & Ibata, R. A. 2018, *MNRAS*, 477, 4063
 —. 2019, *MNRAS*, 486, 2995
 Malhan, K., Ibata, R. A., Carlberg, R. G., Valluri, M., & Freese, K. 2019, *The Astrophysical Journal*, 881, 106
 Malhan, K., Ibata, R. A., & Martin, N. F. 2018, *MNRAS*, 481, 3442
 Mashchenko, S., & Sills, A. 2005, *ApJ*, 619, 243
 Myeong, G. C., Jerjen, H., Mackey, D., & Da Costa, G. S. 2017, *ApJ*, 840, L25
 Navarro, J. F., Frenk, C. S., & White, S. D. M. 1996, *ApJ*, 462, 563
 Peebles, P. J. E. 1984, *ApJ*, 277, 470
 Price-Whelan, A. M., & Bonaca, A. 2018, *ApJ*, 863, L20
 Read, J. I., Iorio, G., Agertz, O., & Fraternali, F. 2017, *MNRAS*, 467, 2019
 Renaud, F., Agertz, O., & Gieles, M. 2017, *MNRAS*, 465, 3622
 Ricotti, M., Parry, O. H., & Gnedin, N. Y. 2016, *ApJ*, 831, 204
 Robin, A. C., Luri, X., Reylé, C., et al. 2012, *A&A*, 543, A100
 Schlegel, D. J., Finkbeiner, D. P., & Davis, M. 1998, *ApJ*, 500, 525
 Shipp, N., Drlica-Wagner, A., Balbinot, E., et al. 2018, *ApJ*, 862, 114
 Watkins, L. L., van der Marel, R. P., Sohn, S. T., & Evans, N. W. 2019, *ApJ*, 873, 118
 Yanny, B., Rockosi, C., Newberg, H. J., et al. 2009, *AJ*, 137, 4377
 Zhao, G., Zhao, Y., Chu, Y., Jing, Y., & Deng, L. 2012, arXiv e-prints, arXiv:1206.3569